Winter 2018
End of Semester Report

by

Austin Schenk

Brigham Young University
April 26, 2018

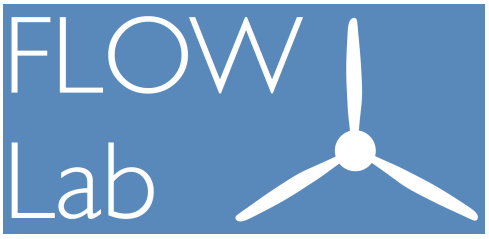

Propeller on Propeller Interactions

Austin R Schenk*
Brigham Young University, Provo, UT, 84602, USA

April 26, 2018

With the advancement of battery technology and more efficient electric motors in aircraft propulsion, non-traditional design configurations must be considered. Distributed propulsion is one configuration that becomes a possibility when using an electric system. In a distributed electric propulsion (DEP) configuration, propellers are densely spread across the wing which introduces complex propeller on propeller interactions. Currently no research has been done on these interactions during forward flight. By creating a computational fluid dynamic (CFD) simulation, using a vortex particle method (VPM) code, and gathering empirical data we aim to model these interactions in relation to separation distance. With an accurate surrogate model we will be able to implement it into existing DEP optimization routines and better propulsion configurations will be achieved.

1 Introduction

Recent advances in batteries and motors have led to drastic changes in what is possible in aircraft design. Aircraft are currently being designed by companies like Boeing and Uber that challenge the traditional design concepts and introduce a myriad of new design considerations. Their current Vertical Take off and Landing (VTOL) air taxi designs take advantage of densely distributing motors and propellers along the span of the wing, however, before any of these conceptual designs can become a reality there needs to be an accompanying advance in research. New models of the complex multi-disciplinary interactions that govern these innovative designs need to be developed and that is the goal of this current research: to fill the gap in knowledge of how closely distributed propellers interact with each other during forward flight.

2 Background

New technology means new possibilities in aircraft design. Only recently has electric powered aviation become a viable direction for future aircraft. Advances in both electric motors and battery power are the key components that are making electric propulsion systems possible in the realm of aerospace. Current electric motors can reach an efficiency of over twice that of standard combustion engines and achieve a specific power of over four times that of standard engines. With the new possibility of changing the most fundamental system of an aircraft, its propulsive systems, there are a myriad of new

Figure 1: Airbus prototype VTOL aircraft.

*Master's Student, Department of Mechanical Engineering

design configurations that must be considered.
However, determining which of the new ideas
will be beneficial and which will not requires
new models, new methods, and deeper understanding of the complex multi-disciplinary interactions that en lace all of aircraft design.

One such potentially beneficial design configuration is that of Distributed Electric Propulsion (DEP). This design configuration consist of densely distributing motors and propellers along the wingspan of the aircraft. Currently, DEP shows great promise, and is key in conceptual aircraft designs that are now seen as the future solution to problems such as urban street congestion. The development of Vertical Takeoff and Landing (VTOL) air taxis has even attracted large companies like Boeing and Uber, however, more modeling and research must be done to consider all of the aspects of such a drastic change of this most fundamental system. Due to this key role that DEP could play in future aircraft designs, understanding these complex interactions is of key importance.

3 Single Propeller Validation Case

With a desire to eventually extend our findings to many flight envelopes and the limits on experimental testing we decided to create a numerical CFD model that would make this possible. A numerical model would allow us to extend our results to larger Reynolds Numbers and different propeller diameter set ups after our base case was validated and verified. Due to the plethora of single propeller empirical data and also the relative simplicity of a single propeller CFD simulation we decided to begin our study here. This would allow refinement of our numerical computer model under computationally less expensive conditions which we could then extend to our multi-propeller cases.

3.1 Empirical Data

The single propeller test cases were all run in the Brigham Young University open return small wind tunnel (see fig 3). The inner dimensions of the wind tunnel are 1.5 x 1.5 x 2.5' and the top speed is 110 mph which was well beyond the range needed for this project. Calibration of the wind tunnel speeds were checked before each set of test using a Testo 416 Mini-Vane hand held anemometer.

3.1.1 Propeller Geometry

Based upon wind tunnel size, test stand limitations, and other inter-lab research extensions we chose to run all our base cases with the APC 4.5x9 Thin Electric propeller. However, due to the proprietary nature of propeller geometries we were unable to get an exact CAD model of the APC 4.5x9 propeller and had to manually digitize the geometry. This was done by cutting the propeller into multiple chord wise sections along the span of the blade. Pictures were then taken of the airfoil sections and fit with standard airfoil data. The twist was also extracted. Then with the twist, span, chord lengths, and airfoil data we were able to create a close geometric approximation of the propeller.

To verify that our propeller geometry used in the CFD simulations was comparable to the actual propeller geometry we printed the propeller to scale. The propeller was 3-D printed in PLA which left a very rough surface, unacceptable for a propeller blade. To smooth the surface it was sanded, coated in primer, and then sanded again multiple times. The end result was a smooth propeller that matched the APC 4.5x9 propeller very closely.

Figure 2: 3-D Printed propeller next to an APC 4.5x9 propeller.

After a visual inspection that the geometries were closely matching, the printed propeller was used in the wind tunnel to compare actual thrust and torque values and good agreement was found(these results can be seen in section 3.3).

3.1.2 Data Collection

To record the torque and thrust produced by the propeller in the wind tunnel we used a single RC-Benchmark 1580 series test stand with its accompanying software which was run on a laptop with a data acquisition rate of 60 Hz. The wind tunnel speeds were calibrated and verified at the beginning of each test set. By maintaining our motor speed at a constant 6900 RPM while varying the wind tunnel velocity from 0-30 m/s we gathered data across the entire advance ratio for our propeller.

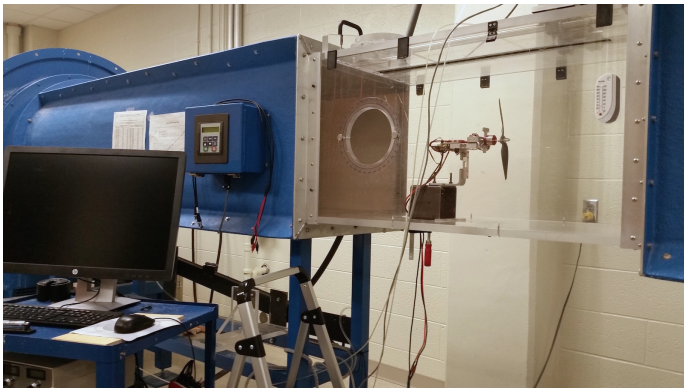

Figure 3: Single propeller wind Tunnel Setup

Once the data was collected, we applied a simple correction to the thrust calculations to account for the drag of the test stand. This was done by simply measuring the drag of the stand at different wind speeds while the propeller was not spinning, fitting a curve to those results and factoring it into the recorded thrust values.

3.1.3 Results

By sweeping our data across the entire advance ratio, applying the wind tunnel corrections (section 3.1.2), and non-dimensionalizing our data we were able to compare our data to existing data. We compared our results to UIUC's propeller database and found good correlation in the data.

3.2 CFD

3.2.1 Grid Convergence Study

By applying general best practice principles to our simulation we created good polyhedral mesh from which we began our grid convergence study. We ran multiple simulations decreasing the base size in the simulation at regular step sizes. We continued this process until our simulation thrust and torque values began to converge. We ran simulations from 900 thousand elements to 16 million elements.

With our results showing a good general spatial convergence we plotted them and applied a Richardson's Extrapolation to estimate our final convergence values (see figure 8). From these results we determined a simulation with approximately 7.8 million cells to be sufficient, which we then applied as a starting mesh for our double propeller simulations.

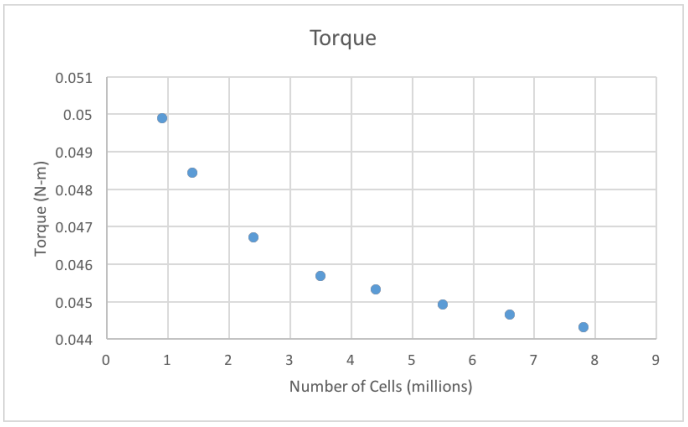

Figure 4: Grid Convergence on Torque value

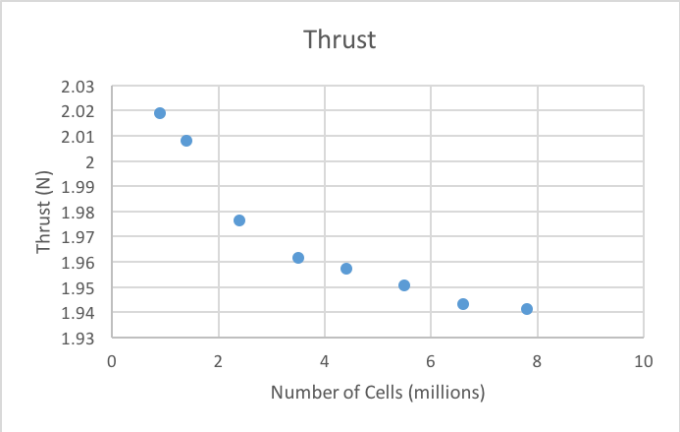

Figure 5: Grid convergence on Thrust Value

3.3 Agreement Between Models

Our CFD values matched our numerical values closely. There is some disagreement in the higher aspect ratios, however this is in part expected due to the steep slope here and the difficulty of resolving those small interactions. With an improved mesh and better wind tunnel correction factors we are confident we could reach even better agreement, but the results below match sufficiently for our purposes.

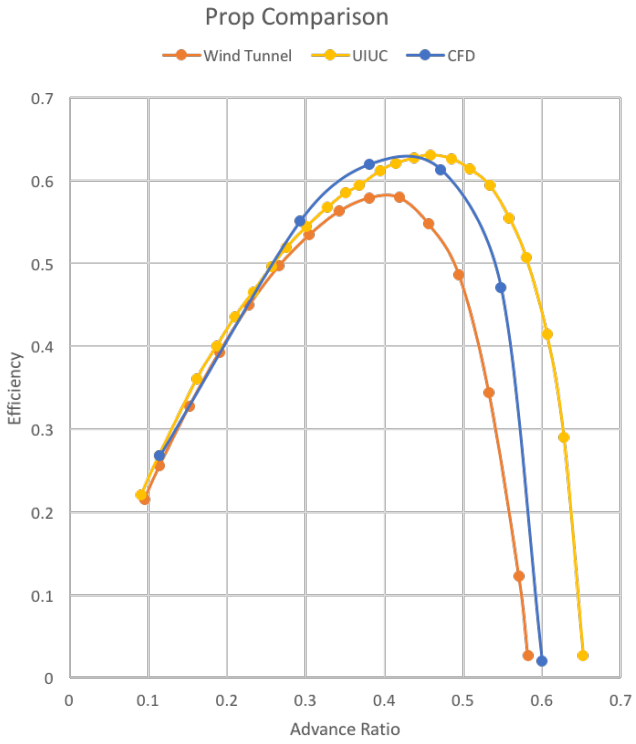

Figure 6: UIUC, CFD, and Wind Tunnel (no corrections) comparison

4 Double propeller Case

With the single propeller case validated and verified we had a good initial starting point for our double propeller simulations. We applied the same mesh parameters and base size to arrive at a starting point. While the single propeller case was a convenient and helpful starting point much refinement was needed to improve the results so that they could be used in validating our VPM code.

4.1 CFD Model

While the single propeller was more of a rough starting point for our models, our double propeller simulations would be the base of our surrogate model and consequently we dove into more depth for them to ensure an accurate model.

Y+: To ensure that we were covering the entire range of Reynold numbers for our simulation we calculated both the boundary layer thickness, the minimum cell size, and the number of prism layers needed. We used the following equations to calculate the Reynolds Number, Boundary layer thickness, minimum prism layer thickness, and number of prism layers needed:

$$Re_{0.75} = \frac{\rho * U_t * C_{0.75}}{\mu}$$

Where U_t is the tangential velocity

$$U_t = \sqrt{w * r_{0.75}^2 + V_\infty^2}$$

From this we determined that the propeller Reynolds Number for max operation conditions would be approximately 200,000.

To calculate the total boundary layer thickness (T) we used the following equation from Schlichting's Empirical solutions.

$$T = \frac{0.37 * C_{0.75}}{Re_{0.75}^{0.2}}$$

Then assuming a Y+ value of 1 we can derive that the initial prism layer must be a thickness of t, where t is the following.

$$t = \frac{C_{0.75}}{Re_{0.75}} \sqrt{\frac{2}{c_f}}$$

To find c_f we assumed a turbulent boundary layer and approximated using Schlichting's Method.

$$C_f = \frac{0.0592}{Re_{0.75}^{0.2}}$$

Then, since StarCCM+ ask for the prism layer information in terms of the number of prism layers, we found the number of layers assuming a growth rate of $s = 1.2$ where n is calculated as follows.

$$n = log_s(\frac{T}{t}(s-1)+1)$$

Once we calculated the above values we input them into our simulation to assure resolution of the entire boundary layer and its related drag.

4.2 Empirical Data

Many of our data collection methods for the double propeller case were very similar to the single propeller case (see section 3.1). Only the wind tunnel and test stand were different.

4.2.1 Wind Tunnel

The double propeller setup would not fit in the smaller wind tunnel that we used for the single propeller case and so all of the double propeller test were run in the large BYU wind tunnel. Due to lack of instrumentation on the newly set up wind tunnel, all wind speed test were done using the same hand held anemometer as before.

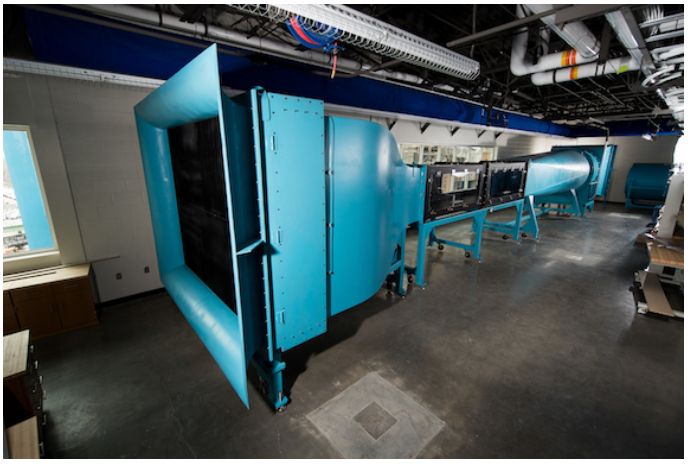

Figure 7: BYU large wind tunnel.

4.2.2 Test Stand Setup

The test stand was made out of 80/20 bar stock that was cut to length and fastened together with bolts and nuts. The 80/20 setup allowed for easy adjustments of the separation distances and for easier attachment to the wind tunnel base plate. The test stand base then had two of the same 1580 RC Benchmarks test stand attached to the top. The wires were run out the bottom and data was recorded once again using two laptops.

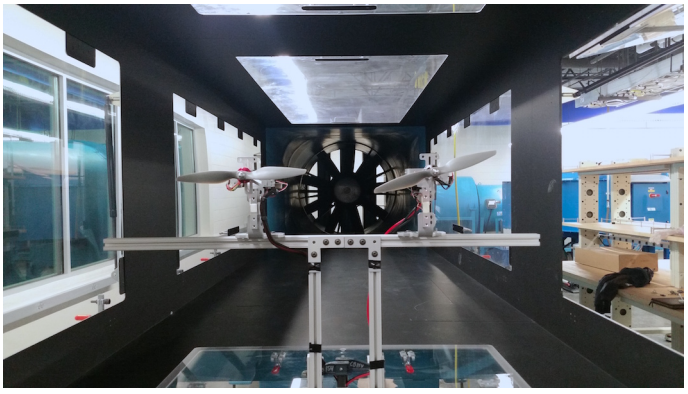

Figure 8: Double Propeller test stand set up.

5 Going forward

The above is much of the base work has been set up for getting results and beginning to create the surrogate model. A finalization of the grid convergence needs to still be done on the CFD from which we will validate the VPM model. With the three methods (CFD, VPM, and Empirical) we will collect data across many different separation distances and flight envelopes. Once all our data is collected we will process it, look for relationships, and attempt to model it mathematically.